

University of Groningen

## Field-ion-microscopy contradiction of the quasicrystal model based on twinning of a cubic crystal

Elswijk, H.B.; Bronsveld, P.M.; Hosson, J.Th.M. De

*Published in:*  
Physical Review B

*DOI:*  
[10.1103/PhysRevB.37.4261](https://doi.org/10.1103/PhysRevB.37.4261)

**IMPORTANT NOTE:** You are advised to consult the publisher's version (publisher's PDF) if you wish to cite from it. Please check the document version below.

*Document Version*  
Publisher's PDF, also known as Version of record

*Publication date:*  
1988

[Link to publication in University of Groningen/UMCG research database](#)

### *Citation for published version (APA):*

Elswijk, H. B., Bronsveld, P. M., & Hosson, J. T. M. D. (1988). Field-ion-microscopy contradiction of the quasicrystal model based on twinning of a cubic crystal. *Physical Review B*, 37(8), 4261-4264. <https://doi.org/10.1103/PhysRevB.37.4261>

### **Copyright**

Other than for strictly personal use, it is not permitted to download or to forward/distribute the text or part of it without the consent of the author(s) and/or copyright holder(s), unless the work is under an open content license (like Creative Commons).

The publication may also be distributed here under the terms of Article 25fa of the Dutch Copyright Act, indicated by the "Taverne" license. More information can be found on the University of Groningen website: <https://www.rug.nl/library/open-access/self-archiving-pure/taverne-amendment>.

### **Take-down policy**

If you believe that this document breaches copyright please contact us providing details, and we will remove access to the work immediately and investigate your claim.

Downloaded from the University of Groningen/UMCG research database (Pure): <http://www.rug.nl/research/portal>. For technical reasons the number of authors shown on this cover page is limited to 10 maximum.

## Field-ion-microscopy contradiction of the quasicrystal model based on twinning of a cubic crystal

H. B. Elswijk, P. M. Bronsveld, and J. Th. M. De Hosson

*Department of Applied Physics, University of Groningen, Materials Science Centre, Nijenborgh 18,  
NL-9747 AG Groningen, The Netherlands*

(Received 30 September 1987)

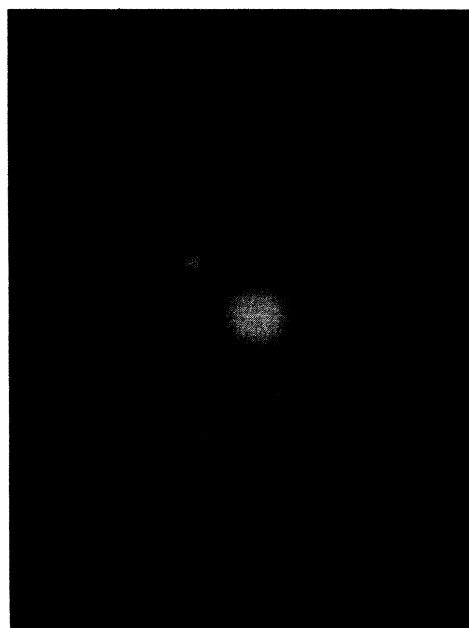
Comparison of computer simulations of field-ion images with experiments clearly shows that twinning of a cubic crystal is not compatible with experimental field-ion microscopic observations of quasicrystals.

The discovery by Shechtman *et al.*<sup>1</sup> of a rapidly quenched Al-Mn alloy giving rise to sharp electron diffraction peaks with fivefold rotation axes initiated a great deal of interest among crystallographers. The apparent icosahedral symmetry involved is incompatible with translational order, but the sharpness of the diffraction peaks points at long-range orientational order. These materials were called quasicrystals. Soon a model had been constructed which at the same time was aperiodic and contained perfect orientational order.<sup>2</sup> This model, the so-called three-dimensional Penrose tiling (3D PT), has the same diffraction pattern as *i*-(Al-Mn). Another approach<sup>3-6</sup> proposes multiple twinning of crystals as a possible explanation of the icosahedral diffraction patterns. A model recently proposed by L. Pauling<sup>6</sup> reproduces high-resolution x-ray powder diffraction patterns, neutron-diffraction experiments, and electron diffraction patterns. Field-ion microscopy (FIM)<sup>7</sup> provides another harsh experimental test to any model, by viewing the material directly in atomic detail. In order to draw conclusions from FIM measurements, however, one has to first calculate the expected image for a modeled structure. In the case of complicated structures it is not sufficient to merely state that twinning is not observed, as in the paper of Melmed and Klein.<sup>8,9</sup> To this end we have performed computer simulations of FIM images both of an undecorated 3D PT and of Pauling's latest model<sup>6</sup> and compared them with experimental images.

The material, an Al<sub>7</sub>Mn<sub>2</sub> alloy, was in the form of ribbons approximately 20  $\mu\text{m}$  thick and 1 mm wide. Small pieces could be polished electrochemically with a mixture of 1.25% of perchloric acid in glacial acetic acid at 5 V dc to produce sharply pointed tips suitable for FIM imaging. The tips were examined in a transmission electron microscope, to ascertain the presence of the icosahedral phase [Figs. 1(a) and 1(b)]. In the FIM an image of the most protruding atoms at the tip surface is created by noble gas ions, ionized in the high electric field region near these atoms, resulting from a high voltage supplied to the tip.<sup>7</sup> Pencil beams of ions accelerated approximately radially from the tip strike the detector where the ion current is converted into an electron current with an amplification of  $10^6$  times. These electrons cause scintil-



(a)



(b)

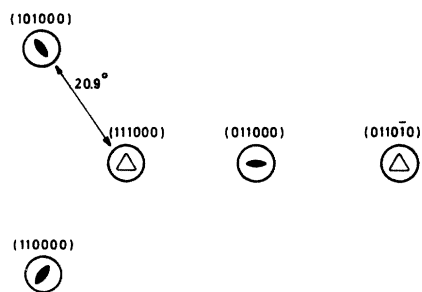
FIG. 1. (a) Dark-field transmission electron microscopy (TEM) image of an Al<sub>7</sub>Mn<sub>2</sub> FIM tip; a grain with a fivefold axis is imaged brightly. (b) The electron diffraction pattern of the grain depicted in (a).



(a)



(b)



(c)

FIG. 2. (a), (b) Helium images of an  $\text{Al}_7\text{Mn}_2$  icosahedral tip at about 15 K, (a) at 11 kV, (b) at slightly higher voltage. Distance across images is approximately 50 nm. (c) Index map of the observed poles.

lations on a phosphorescent screen which can be recorded photographically or with a video camera. The specimen was cooled to 15 K by a He gas flow cryostat and the background pressure was  $2 \times 10^{-10}$  Torr. Helium was used as the imaging gas at a pressure of  $1 \times 10^{-5}$  Torr. By field evaporation of irregularities, the tip is smoothed to an atomic level. Imaging with helium often leads to fracture of the very brittle material, caused by the high electric field necessary to ionize helium, which results in a tensile stress. Imaging with neon, however, with a lower electric field at the tip, did not give satisfactory results. Figures 2(a) and 2(b) depict images of a specimen with a threefold axis near the optical axis of the microscope. The applied voltage was approximately 11 kV and the tip to screen distance, which together with the tip radius determines the magnification,<sup>7</sup> was 53 mm. The form of this particular tip appeared to be ellipsoidal rather than hemispherical as a result of the ribbonlike original form of the material that was electropolished. In this case the magnification depends on the direction parallel to the tip surface. This effect leaves the observed angles unchanged. Indexing according to the six vectors pointing at six vertices of an icosahedron:  $\mathbf{q}_1 = (\tau, 0, 1)$ ,  $\mathbf{q}_2 = (\tau, 0, -1)$ ,  $\mathbf{q}_3 = (1, \tau, 0)$ ,  $\mathbf{q}_4 = (0, 1, \tau)$ ,  $\mathbf{q}_5 = (0, -1, \tau)$ ,  $\mathbf{q}_6 = (1, -\tau, 0)$ , with  $\tau = (\sqrt{5} + 1)/2$  being the golden mean, we clearly observe the (111 000) pole surrounded by three twofold poles: (101 000), (110 000), and (011 000); see Fig. 2(c). In some micrographs the (011 010) threefold pole is also visible, while evidence of the presence of {100 000} fivefold poles is absent. The poles are expected  $37^\circ$  away from the central (111 000) pole. Imaging characteristics at the edge of the image are rather poor, but a prominent pole would have been noticed during the course of field evaporation. The prominence of poles in field-ion micrographs of crystals is associated with the interplanar distance of the planes concerned.<sup>7</sup> This would indicate larger interplanar distances along threefold and twofold axes than along fivefold ones. The measured angles are, within the accuracy of the technique, compatible with icosahedral symmetry. Figure 3 shows computer simulations of an undecorated 3D PT. This tiling is generated by the "cut and projection method."<sup>10</sup> The vertices which lie within a spherical shell of radius 200 times the rhombohedral edge length and thickness 0.1 edge lengths are projected stereographically onto a plane. Computer simulations of this kind<sup>11</sup> have proved to be very helpful in interpreting FIM images. Figure 3(a) depicts a fivefold orientation whereas 3(b) shows a threefold pole in the center, as in our experimental observations. Qualitatively the simulations agree very well with experiment. Poles appear at the right positions and quasilattice planes exist and extend to large enough areas to form circles of edge atoms. The experimental observations, however, appear more chaotic than simulations predict. This observation is largely due to preferential ionization or evaporation<sup>7</sup> of one of the alloyed species as confirmed with FIM micrographs of a crystalline  $\text{Al}_4\text{Mn}$  sample (Fig. 4). Only the most prominent poles are imaged as areas of concentric ring structures, while high-index regions appear amorphous. These image characteristics of disordered alloys are well known

from FIM literature<sup>7</sup> and greatly limit the usefulness of the technique applied to alloys. Nevertheless, on the basis of our observations in comparison with a simulation of a FIM image of the structure proposed by Pauling<sup>6</sup> we can now positively exclude his model based on twinning of cubic crystals of large unit cells. The simulated FIM image of a sample with this structure having a tip radius of 50 nm is depicted in Fig. 5. We calculated all atom positions within the 820-atom unit cell from the positions of a slightly deformed Friauf polyhedron<sup>12</sup> of which 20 in-

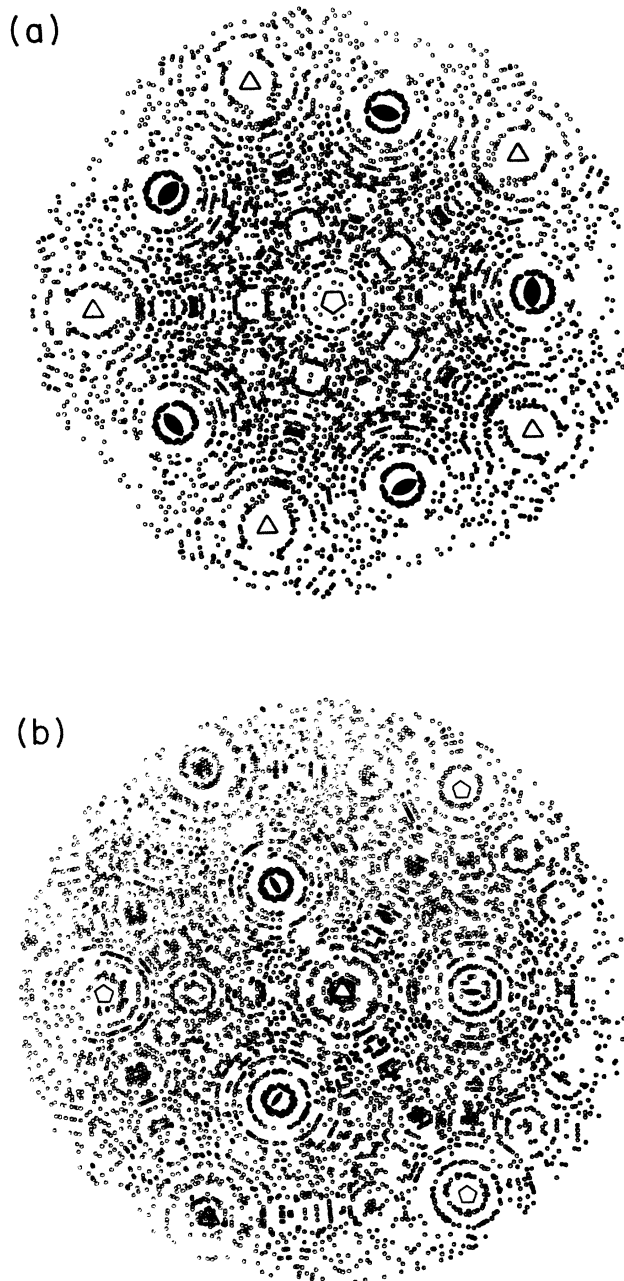


FIG. 3. Simulations of FIM images of an undecorated 3D Penrose tiling. (a) Fivefold orientation and (b) threefold orientation. Poles are marked with symmetry elements. Radius of tip is 200 rhombohedral edge lengths.

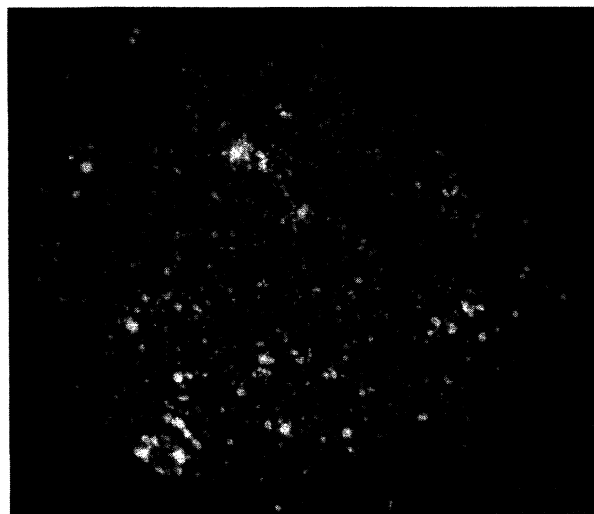


FIG. 4. Helium image of a crystalline  $\text{Al}_4\text{Mn}$  sample. Angular distance from lower left to upper right pole is about  $90^\circ$ . Distance across is approximately 60 nm.

terpenetrating atoms form a complex. The polyhedron has to be deformed in order to fit in a solid angle of  $4\pi/20$  sr.

The exact positions we used for the atoms in the Friauf polyhedron are  $\mathbf{a}_1 = (\tau, 0, 1)$ ,  $\mathbf{a}_2 = (1, \tau, 0)$ ,  $\mathbf{a}_3 = (0, 1, \tau)$ ,  $\mathbf{a}_4 = f_1 \mathbf{a}_1$ ,  $\mathbf{a}_5 = f_1 \mathbf{a}_2$ ,  $\mathbf{a}_6 = f_1 \mathbf{a}_3$ ,  $\mathbf{a}_7 = \mathbf{a}_4 + f_2 \mathbf{a}_2$ ,  $\mathbf{a}_8 = \mathbf{a}_4 + f_2 \mathbf{a}_3$ ,  $\mathbf{a}_9 = \mathbf{a}_5 + f_2 \mathbf{a}_1$ ,  $\mathbf{a}_{10} = \mathbf{a}_5 + f_2 \mathbf{a}_3$ ,  $\mathbf{a}_{11} = \mathbf{a}_6 + f_2 \mathbf{a}_1$ ,  $\mathbf{a}_{12} = \mathbf{a}_6 + f_2 \mathbf{a}_2$ , and  $\mathbf{a}_{13} = \frac{1}{12} \sum_{i=1}^{12} \mathbf{a}_i$ , where  $f_1 = [2 + (1 + \tau^2)^{1/2}] / (1 + \tau^2)^{1/2}$  and  $f_2 = 2(1 + \tau^2)^{1/2}$ . Note that the inner three positions of this polyhedron ( $\mathbf{a}_1, \mathbf{a}_2, \mathbf{a}_3$ ) together with nine other positions all shared by

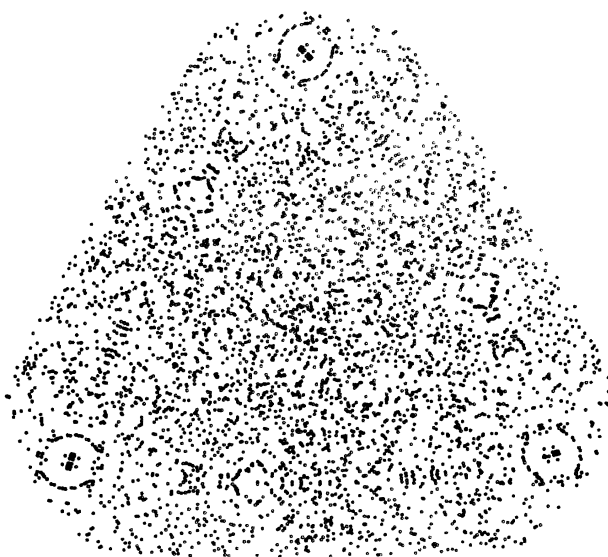


FIG. 5. Simulation of a FIM image of a crystal in (111) orientation with an 820-atom unit cell as proposed by Pauling (Ref. 6). Three  $\{100\}$  poles are visible. Distance across about 60 nm.

five polyhedra, form a central icosahedron. Atoms at  $\mathbf{a}_4$ ,  $\mathbf{a}_5$ , and  $\mathbf{a}_6$  are part of a second, larger icosahedron around the inner one.  $f_1$  makes the distance from atom 1 to atom 4, equal to that from atom 1 to atom 2. Positions  $\mathbf{a}_7$ – $\mathbf{a}_{12}$  form an irregular hexagon. Twenty of these polyhedra form a complex. Scaling of this complex is achieved by the requirement that two  $C_2$  complexes share two atoms. This means that  $\|\mathbf{a}_7 + \mathbf{a}_8\| = 2.336/2$  nm, 2.336 nm being the unit-cell edge length,<sup>6</sup> hence all coordinates must be multiplied by 0.1166 nm. This complex repeats in the cubic unit cell conforming to the  $\beta$ -W structure. In this simulation a larger solid angle is observed, in order to show that only  $\{100\}$  poles show prominent features. The image as a whole reveals far less structure than observed experimentally, and this observation alone justifies the exclusion of Pauling's model. A FIM image of a tip composed of several twinned regions would result in a "patchwork" of patches already observable in our single-crystal simulation, conceivably not improving overall regularity. Thus, twinning would result

in even less-ordered images. The disordered appearance of this simulation can be understood as a consequence of the incompatibility of the cubic crystal structure with the internal structure in the large unit cell. Even within the cell, e.g.,  $\{111\}$  planes defined by  $C_1$  complexes<sup>6</sup> do not coincide with similar planes of  $C_2$  complexes. This results in effectively small interplanar distances and absence of densely packed planes extending to large areas without interruption. Because the prominence of poles and existence of concentric ring patterns depend on these interplanar distances, FIM is very sensitive to these features, more so than diffraction techniques. In conclusion we can state that all models claiming to reproduce experimental measurements must have densely packed planes perpendicular to the twofold and threefold axes of the icosahedral symmetry extending to at least 50 nm distance. The latest model of L. Pauling, based on twinning of a crystal with a large unit cell, does not satisfy this demand. Models based on decoration of a 3D PT are better candidates with respect to this requirement.

<sup>1</sup>D. Shechtman, I. Blech, D. Gratias, and J. W. Cahn, *Phys. Rev. Lett.* **53**, 1951 (1984).

<sup>2</sup>D. Levine and P. J. Steinhardt, *Phys. Rev. Lett.* **53**, 2477 (1984).

<sup>3</sup>L. Pauling, *Nature (London)* **317**, 512 (1985).

<sup>4</sup>R. D. Field and H. L. Fraser, *Mater. Sci. Eng.* **68**, L17 (1984–1985).

<sup>5</sup>M. J. Carr, *J. Appl. Phys.* **59**, 1063 (1986).

<sup>6</sup>L. Pauling, *Phys. Rev. Lett.* **58**, 365 (1987).

<sup>7</sup>E. W. Müller and T. T. Tsong, *Field Ion Microscopy: An Introduction to Principles, Experiments and Applications* (American

Elsevier, New York, 1969).

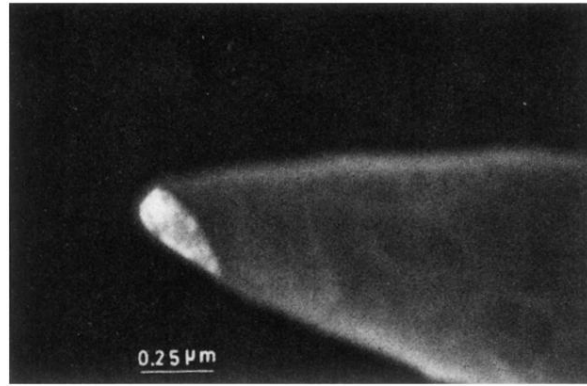
<sup>8</sup>A. J. Melmed and R. Klein, *Phys. Rev. Lett.* **56**, 1478 (1986).

<sup>9</sup>J. W. Cahn, D. Gratias, and D. Shechtman, *Nature (London)* **319**, 102 (1986).

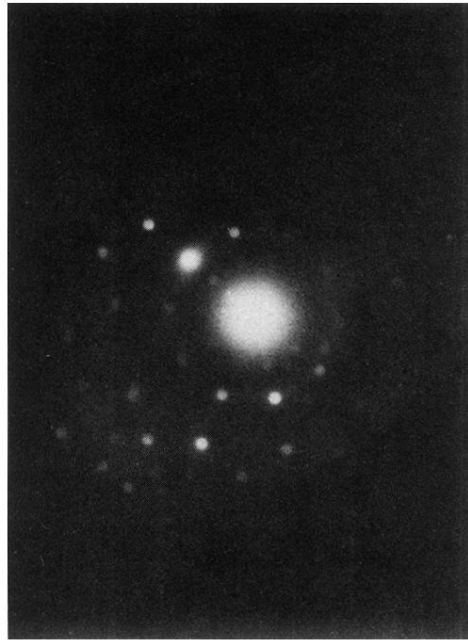
<sup>10</sup>Veit Elser, *Acta Crystallogr., Sect. A* **42**, 36 (1986).

<sup>11</sup>A. J. W. Moore and S. Ranganathan, *Philos. Mag.* **16**, 723 (1967).

<sup>12</sup>S. Samson, in *Structural Chemistry and Molecular Biology*, edited by A. Rich and N. Davidson (Freeman, San Francisco, 1968), pp. 687–717.

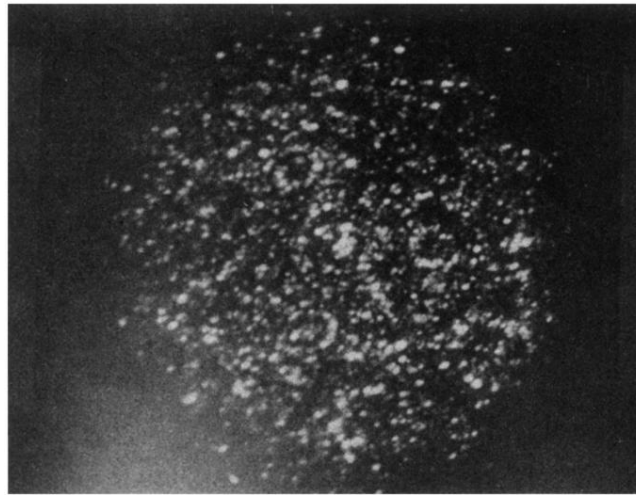


(a)

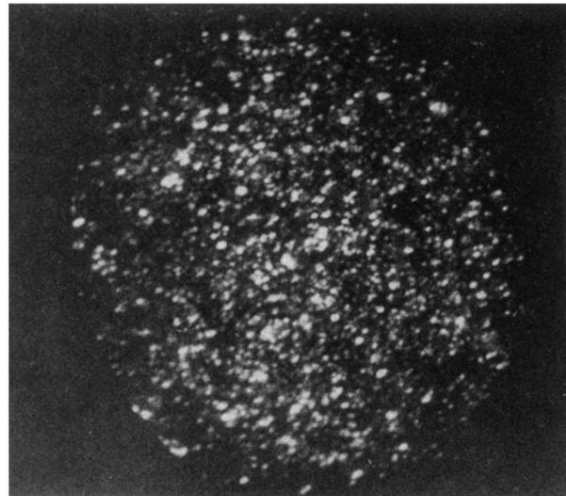


(b)

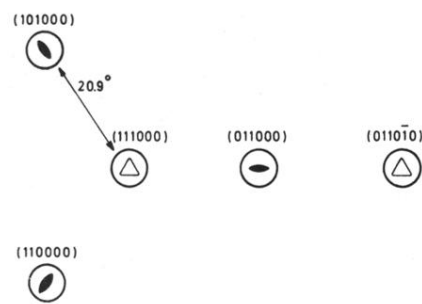
FIG. 1. (a) Dark-field transmission electron microscopy (TEM) image of an  $\text{Al}_7\text{Mn}_2$  FIM tip; a grain with a fivefold axis is imaged brightly. (b) The electron diffraction pattern of the grain depicted in (a).



(a)



(b)



(c)

FIG. 2. (a), (b) Helium images of an  $\text{Al}_7\text{Mn}_2$  icosahedral tip at about 15 K, (a) at 11 kV, (b) at slightly higher voltage. Distance across images is approximately 50 nm. (c) Index map of the observed poles.

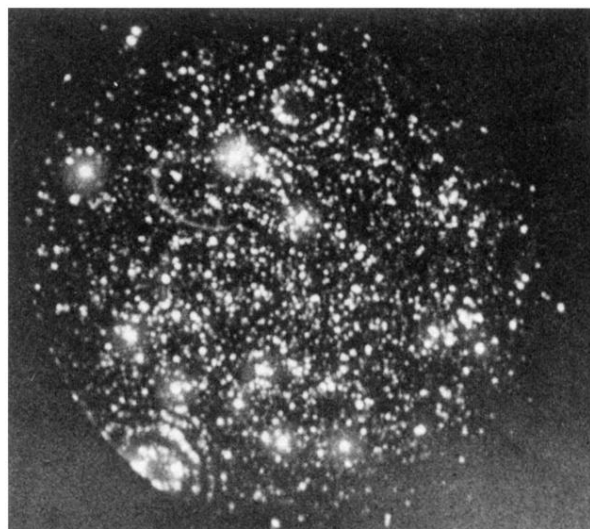


FIG. 4. Helium image of a crystalline  $\text{Al}_4\text{Mn}$  sample. Angular distance from lower left to upper right pole is about  $90^\circ$ . Distance across is approximately 60 nm.